Sensors and Materials, Vol. 16, No. 2 (2004) 085–098
MYU Tokyo

S & M 0549

Optomechanical Characterization of Mechanically Deflected Free-Standing Polymer Waveguides

Young-Hyun Jin, Moo-Jin Choi and Young-Ho Cho*

Digital Nanolocomotion Center
Korea Advanced Institute of Science and Technology
373-1 Gusong-dong, Yusong-gu, Daejon 305-701, Republic of Korea

(Received January 7, 2004; accepted February 16, 2004)

Key words: optical loss, polymer waveguide, free-standing waveguide, integrated optics

We characterize the micro-optomechanical properties and behavior of mechanically deflected free-standing polymer waveguides. The total optical loss of the mechanically deflected waveguides is evaluated, including propagation loss, input/output coupling loss, geometric curvature loss and mechanical bending loss. Three different sets of polymer waveguides are designed, fabricated and tested: straight waveguides for propagation and coupling loss measurement; curved waveguides for curvature loss measurement; free-standing waveguides for mechanical bending loss measurement. From the straight and curved waveguides, the propagation loss has been measured as 5.4±1.1 dB/cm with the coupling loss of 5.3±2.4 dB, and curvature loss as 4 dB/rad in maximum value, respectively. The mechanical bending loss, measured by the waveguide bending test, rapidly increased to the range of 12–25 dB for the waveguide deflection beyond the elastic region. The reason for the rapid increase of the mechanical bending loss in the large deflection region can be explained as being due to the abrupt change of propagation angles as well as the mechanical defect generated in the waveguides. Furthermore, the elastic limit of the polymer waveguide has been observed at 5±1 MPa, and the failure strength has been measured as 23±8 MPa from the waveguide bending test.

1. Introduction

Recently, micro-electro-mechanical systems (MEMS)-based integrated microoptics[1–5] has received increasing attention for application to information and optical communication systems. Among the devices, a monolithic-integrated optical pickup[1,2] shows strong

*Corresponding author, e-mail address: nanosys@kaist.ac.kr

potential for high-density optical storage devices. For the integrated optical devices, we require appropriate methods to interconnect the movable optical components, such as pickups with stationary components such as light sources. Feasible optical interconnections can be provided by fiber-optic cables, waveguide cables, or waveguide channels on a flexible ribbon. For more compact and simple applications, we propose free-standing (or suspended) waveguides (Fig. 1) not only for the optical interconnection but also for the micromechanical suspension. Therefore, an understanding of the micromechanical behavior and optical characteristics of a movable free-standing waveguide is required for the successful development of monolithic integrated optical devices.

In previous research works,[6–8] optical loss caused by the geometric curvature change of optical fibers and waveguides has been studied. The optical loss caused by the refractive index change due to mechanical stress has been investigated by Nagano, *et al.*[9] This is the first attempt, however, to characterize the optomechanical behavior of a mechanically deflected free-standing polymer waveguide. In addition to the propagation loss and the curvature loss, we particularly focus on the mechanical bending loss, generated by the stress and the curvature change due to the waveguide deflection.

2. Design of Polymer Waveguide Test Structures

Total optical loss in the mechanically deflected free-standing waveguide (Fig. 1) consists of propagation loss, input/output coupling loss, geometric curvature loss and mechanical bending loss. The mechanical bending loss in a deflected waveguide is composed of 1) stress loss, caused by the stress-induced optical refractive index change, 2) angle loss, caused by an abrupt change of propagation directions, and 3) other optomechanical

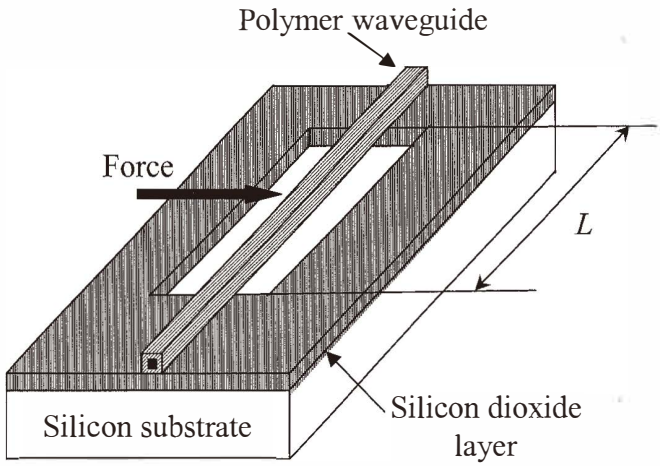

Fig. 1. Perspective view of a free-standing waveguide beam.

losses of crack, defects, or imperfections, generated by an excess mechanical deflection of the waveguides. Three types of waveguide test structures are designed and fabricated to characterize these loss components.

Figure 2 shows a cross section of free-standing polymer waveguides. BisbenzoCycloButene (BCB), UV15 and UV15LV are used as the core, the upper cladding and the lower cladding materials for the polymer waveguide, respectively. The material properties of each layer are listed in Table 1.

Figure 3(a) shows the test structures for the propagation and coupling loss measurement. A simple cut-back method has been used for the direct measurement of the propagation loss.

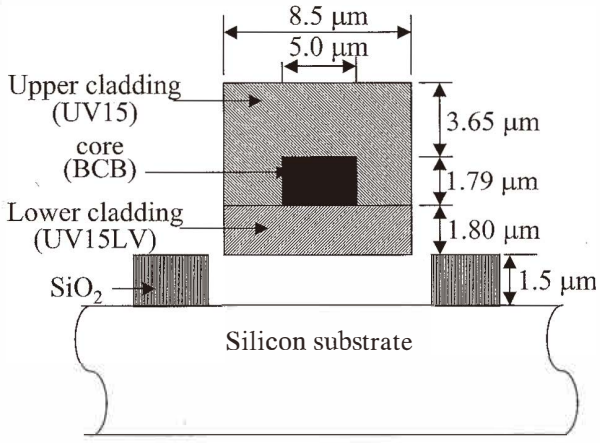

Fig. 2. Cross-sectional view and dimensions of the free-standing polymer waveguide of Fig. 1.

Table 1
Material properties of the polymer waveguide.

Layer (material)	Refractive index (@ 1330 nm)	Young's modulus	Poisson's ratio
Core (BCB8[10])	1.5447	2.0 GPa	0.34
Lower cladding (UV15LV[11])	1.5043	0.8 GPa	0.34
Upper cladding (UV15[11])	1.5043	0.9 GPa	0.34
SiO_2 (Thermal oxide)	1.4469	73 GPa	0.17

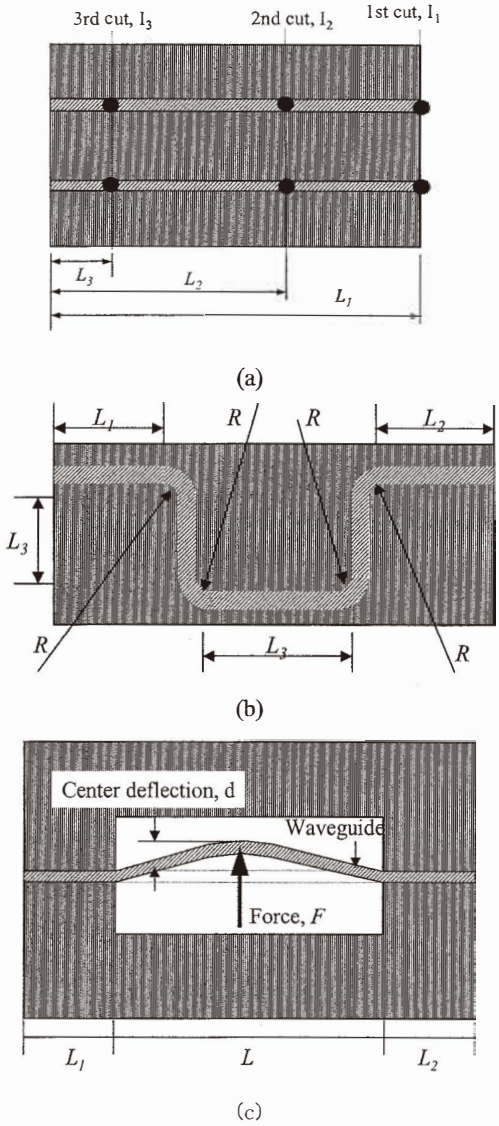

Fig. 3. Schematic view of test structures: (a) test structure for propagation loss measurement; (b) test structure for curvature loss measurement; (a) test structure for mechanical bending loss measurement.

The geometric curvature loss is measured from the test structures shown in Fig. 3(b). Each structure consists of five pieces of straight waveguide and four segments of curved waveguide of an identical radius of curvature, including 100 μm, 200 μm, 300 μm, 400 μm,

800 μm, 1200 μm, 1600 μm and 2000 μm. After measuring the total insertion loss of the test structure, we evaluate the curvature loss by subtracting the propagation and coupling losses from the total insertion loss.

The bending loss test structure is shown in Fig. 3(c). The total length of the free-standing waveguide, *L*, is designed as 1,700 μm and 4,600 μm. The optical loss of the test structure is measured for a varying deflection at the center of the fixed free-standing waveguide.

3. Fabrication of Polymer Waveguide Test Structures

A set of waveguide test structures has been fabricated by the 3-mask surface micromachining process illustrated in Fig. 4. As shown in Fig. 4(a), we grow a 1.5-μm-thick wet SiO_2 film on the silicon wafers. Spin coating and UV curing processes define a

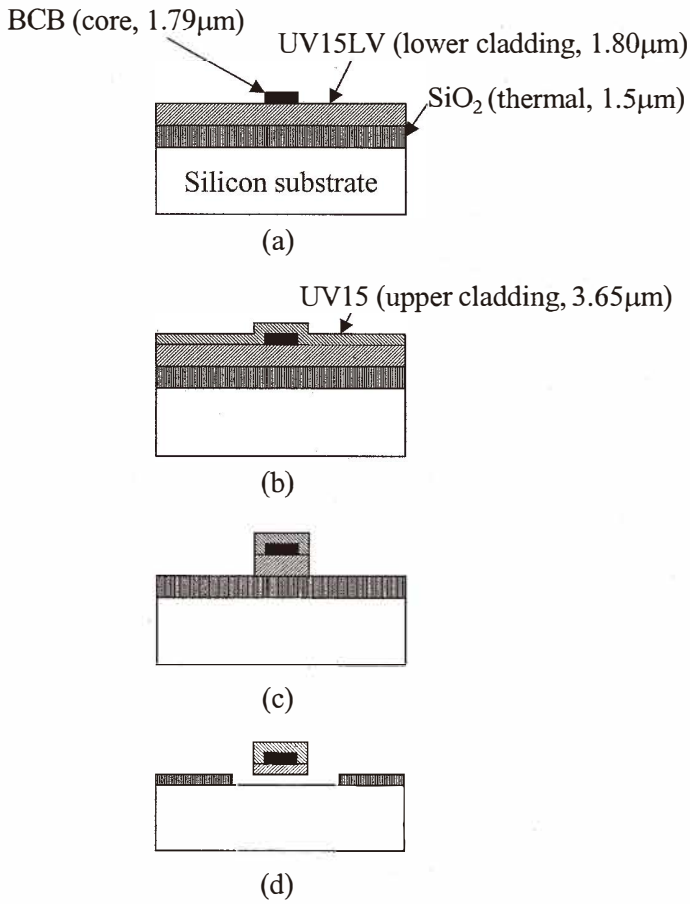

Fig. 4. Microfabrication process for the free-standing polymer waveguide.

1.80-μm-thick polymer (UV15LV) lower cladding layer on the thermal oxide layer. Then, a 1.79-μm-thick BCB polymer core layer is coated and thermally cured on the UV15LV layer. The waveguide core is patterned by the reactive ion etching (RIE) process using a photoresist (PR) mask. As shown in Fig. 4(b), a 3.65-μm-thick UV15 polymer layer is coated as an upper cladding. The waveguide cladding is patterned (Fig. 4(c)) by the RIE process using a metal mask. The free-standing waveguide is obtained (Fig. 4(d)) by removing the thermal oxide layer under the waveguide using a buffered oxide etcher (BOE) and a thick PR mask. Figure 5 shows three different types of test structures, including the straight, curved and free-standing waveguides.

4. Optomechanical Analysis

In this work, we assume that the mechanical bending loss includes three loss components: 1) stress loss; 2) angle loss; 3) other optomechanical losses. For the theoretical analysis of the first two loss components, the mode profile in the fabricated waveguide is measured as a 6.90-μm-wide and 4.61-μm-high Gaussian beam.

4.1. *Stress loss*

The stress loss comes from the internal reflection and the mode conversion due to the stress-induced refractive index change in the waveguide. The relationship between the principal refractive indices and the principal stresses[12] determines the refractive index change.

$$n_1 = n_0 + C_1\sigma_1 + C_2(\sigma_2 + \sigma_3) \tag{1}$$

$$n_2 = n_0 + C_1\sigma_2 + C_2(\sigma_3 + \sigma_1) \tag{2}$$

$$n_3 = n_0 + C_1\sigma_3 + C_2(\sigma_1 + \sigma_2) \tag{3}$$

Here, n_0 is the original refractive index of the material and n_i and s_i are the changed principal refractive indices and principal stresses, respectively. C_1 and C_2 are material constants. The stress-optic or photoelastic constant, C, defined as $C=C_1-C_2$ for the polymer epoxy resin at room temperature, is approximately 56×10^{-12} m^2/N.[13]

The refractive index change in the axial direction caused the reflection loss. When the optical wave propagates into the higher refractive index portion, the light is reflected, thus generating reflection loss, L_{ref}, as follows.

$$L_{ref} = -10 \times \log(1-Re)[\mathrm{dB}] \tag{4}$$

Here, the reflectance, Re, is defined as

$$Re = \left(\frac{n_2 - n_1}{n_2 + n_1}\right)^{1/2} \tag{5}$$

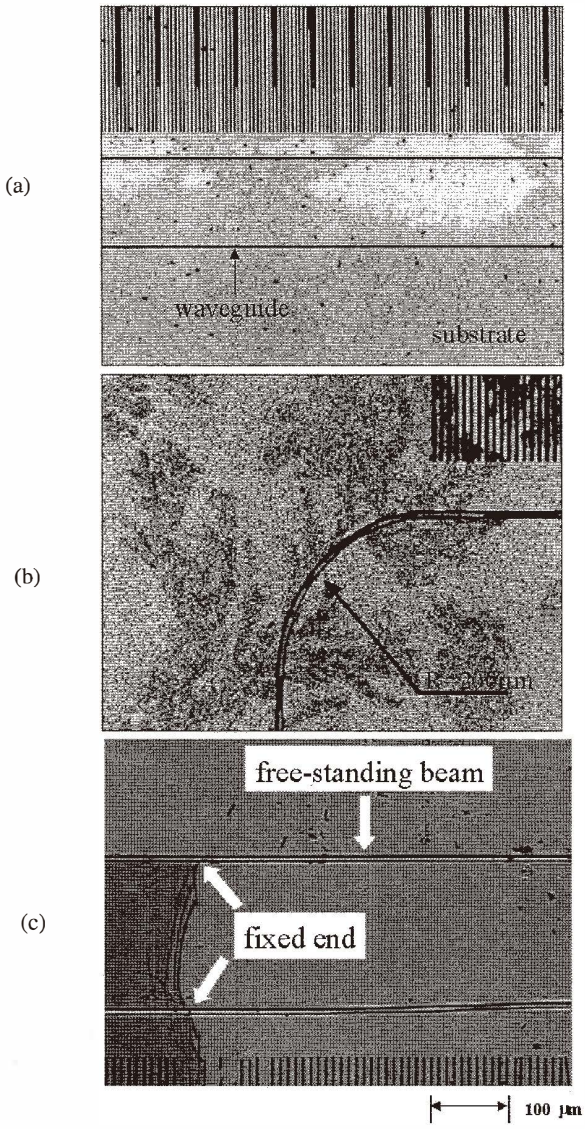

Fig. 5. Fabricated test structures: (a) straight waveguide; (b) curved waveguide; (c) free-standing waveguide beam.

Both n_1 and n_2 are indicated in eqs. (1) and (2).

For a given refractive index distribution in the width direction, the peak of the optical wave moves to the higher refractive index region, thus causing the mode conversion due to the mode mismatch. The mode mismatch loss can be expressed as follows.

$$L_{conv} = -10 \times \log(1 - \eta) \tag{6}$$

where

$$\eta = \frac{\int\int E_1 \cdot E_2 dA}{|E_1 \cdot E_2|} \tag{7}$$

In eq. (7), E_1 and E_2 are the mode distributions at the original and modified refractive index distributions, respectively.

From the tensile strength of the waveguide, the maximum refractive index change in the waveguide is estimated as 0.005. From eq. (6), the maximum internal reflection loss is calculated as 1.6×10^{-5} dB. From BPM simulation, the maximum mode conversion loss is estimated as 5.4×10^{-3} dB.

4.2. *Angle loss*

For a large waveguide deflection, the deflected shape of the waveguide is no longer a smooth one. The abrupt angle change caused by the plastic deformation of the deflected waveguide increases radiation loss, called "angle loss." The angle loss due to the light direction change is also estimated from the Beam Propagation Method (BPM) analysis using the bent waveguide model shown in Fig. 6. The bent angle (q in Fig. 6) of the waveguide is obtained from the bending test of the free-standing waveguide by measuring the center deflection of the deflected waveguide (Fig. 7). The estimated angle loss versus the center deflection (d in Fig. 3(c)) is shown in Fig. 8.

5. Experimental Measurement and Characterization

A laser diode, λ=1330 nm, is used as a light source attached to the end of the waveguide for optical loss measurement. The averaged propagation loss of 5.4±1.1 dB/cm and the averaged coupling loss of 5.3±2.4 dB are measured from ten measurements of six different propagation loss test structures.

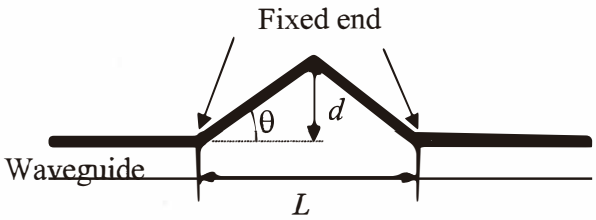

Fig. 6. BPM simulation model for the measurement of angle loss in the best waveguide.

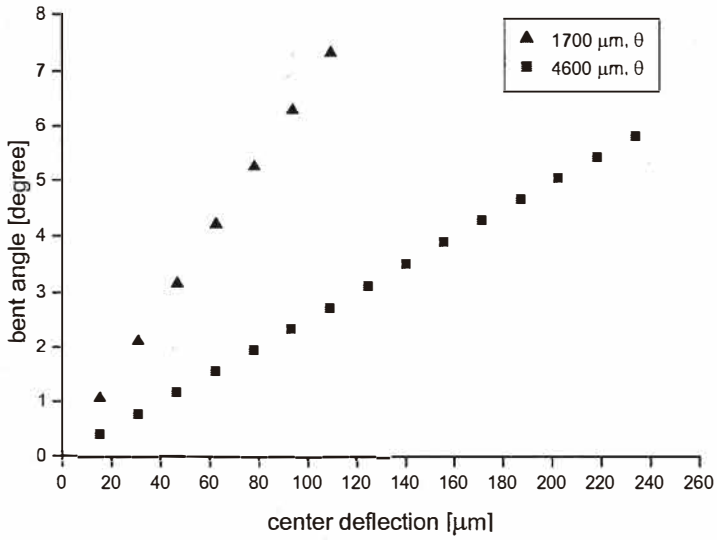

Fig. 7. Bent angle (q in Fig. 6) of the free-standing waveguide with respect to the center deflection.

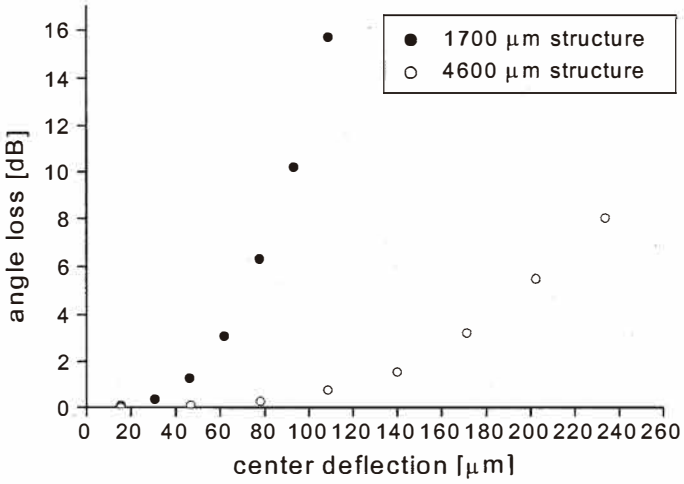

Fig. 8. Estimated angle loss with respect to the center deflection (d in Fig.3(c)).

Figure 9 shows the measured curvature loss. The curvature loss is obtained by subtracting the propagation and coupling losses from the measured total insertion loss of the curved waveguide test structure. Figure 9 shows the measured curvature loss from the ten measurements of the total loss with measurement error of ±1.2 dB/rad. The curvature loss can be neglected for the radius larger than 800 μm. For the radius smaller than 800 μm, the curvature loss increases slightly.

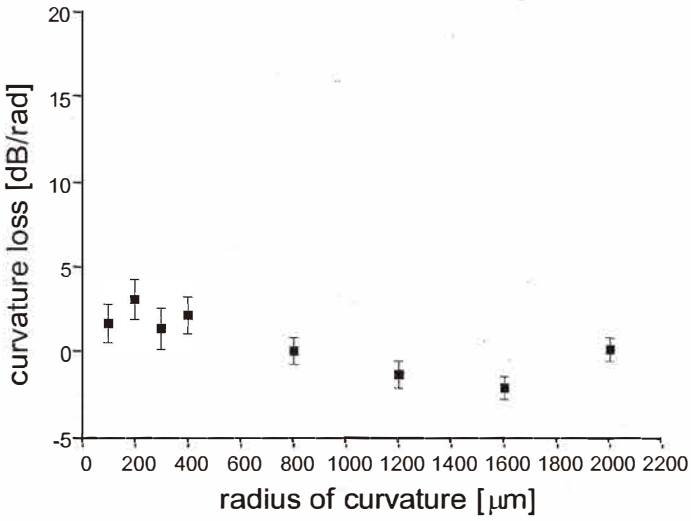

Fig. 9. Measured geometric curvature loss.

From the waveguide bending test, we observe the onset point of the permanent deformation at 25 μm (center deflection) in the 1700-μm-long free-standing waveguide and at 125 μm in the 4600-μm-long free-standing waveguide. The elastic limit of the polymer waveguide is found as 5±1 MPa from the tresca stress (one of the yield criteria) calculated by finite element method (FEM) analysis. In addition, the failure strength is estimated as 23±8 MPa.

The mechanical bending loss is obtained by extracting the propagation loss, coupling loss and geometric curvature from the optical loss measured from the mechanical bending test of the suspended waveguides. Figure 8 shows the results. We find that the mechanical bending loss rapidly increases to 12–25 dB for the waveguide deflection beyond the elastic region. The stress loss, estimated in the range of 1.6×10^{-5} dB – 5.4×10^{-3} dB in the previous section, is negligible compared to the propagation loss. We consider that the reason for the rapid increase of the mechanical bending loss in the large deflection region (i.e., plastic deformation region) is the geometric optical loss caused by the abrupt change of propagation angle (angle loss). The measured mechanical bending loss is compared with the estimated angle loss in Fig. 10. For the case of a 4,600-μm-long structure, the calculated angle loss becomes smaller than the measured mechanical bending loss in the large deflection region. The discrepancy is due to the additional optomechanical loss, caused by the defects generated in the deflected waveguide.

6. Conclusion

In this paper, we characterized the micro-optomechanical behavior of the free-standing polymer waveguide subject to mechanical deflection. We designed and fabricated three

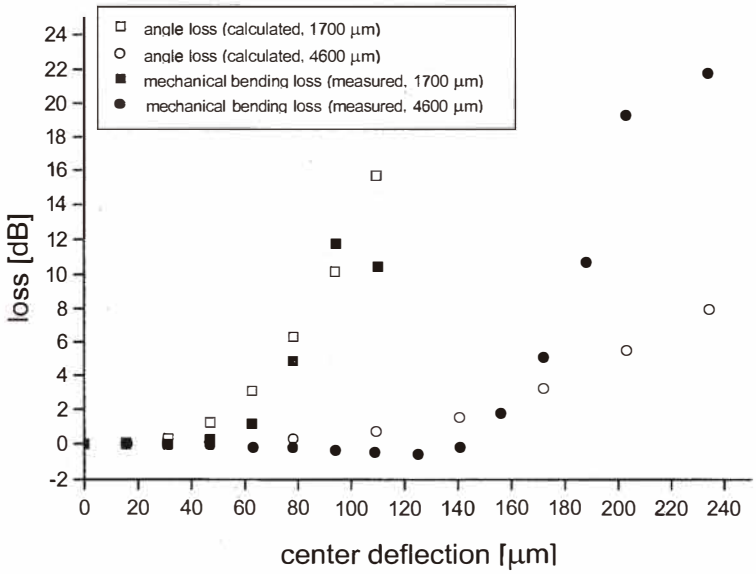

Fig. 10. Comparison of the measured mechanical bending loss and the estimated angle loss.

types of test structures for the measurement of the propagation loss, curvature loss and mechanical bending loss. The propagation loss and the coupling loss of the straight waveguide were measured as 5.42±1.12 dB/cm and 5.32±2.38 dB, respectively. We measured the curvature loss of the curved waveguides as 4 dB/rad in the radius range of 100–2000 μm. The mechanical bending loss, obtained from the bending test of 1,700-μm- and 4,600-μm-long free-standing waveguides, rapidly increased to 12–25 dB for the large waveguide deflection. The sharp increase of the mechanical bending loss in a large deflection region was caused by the abrupt change of propagation directions as well as by the mechanical defects generated in the waveguides. Furthermore, from the bending test of a free-standing waveguide, the elastic limit and the failure strength of the polymer waveguide were measured as 5±1MPa and 23±8MPa, respectively.

Acknowledgments

This work has been supported by the National Creative Research Initiative Program of the Ministry of Science and Technology (MOST) under the project title of "Realization of Bio-Inspired Digital Nanoactuators." The authors would like to acknowledge the technical discussion and assistance provided by Professor Sang-Yung Shin and researchers at the Electooptics Laboratory, Department of Electrical Engineering, KAIST.

References

1 S. Ura, T. Suhara, H. Nishihara and J. Koyama: J. Lightwave Technology **4** (1986) 913.
2 T. Suhara, H. Nishihara and J. Koyama: Opt. Commun. **19** (1976) 353.
3 M. Miler and M. Skalsky: Opt. Commun. **33** (1980) 13.
4 H. Nishihara, M. Haruna and T. Suhara: Optical Integrated Circuits (McGraw-Hill 1989) p. 355.
5 I. Shubin and P.L.K Wa: Electronics Letter **37** (2001) 451.
6 D. Marcuse: Bell Syst. Tech. J. **50** (1971) 2551.
7 E. A. J. Marcatili: Bell Syst. Tech. J. **48** (1969) 2103.
8 W. J. Minford, S. K. Korotky and R. C. Alferness: IEEE Journal of Quantum Electronics **10** (1982) 1802.
9 K. Nagano, S. Kawakami and S. Nishida: Applied Optics **17** (1978) 2080.
10 Processing Procedures for Dry-Etch Cyclotene Advanced Electronics Resins (Dry-Etch BCB), Dow Chemical Company, pp. 1–6.
11 Master Bond UV curable product selector guide, C228–C229.
12 H. Abend and C. Guillemet: Photoelasticity of Glass (Springer-Verlag, 1993) p. 56.
13 A. Kushe and G. Robertson: Photoelastic Stress Analysis (John Wiley & Sons, 1974) p. 152.

About the Authors

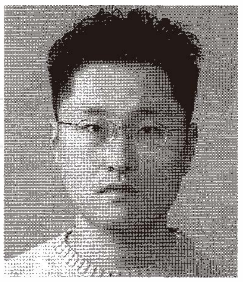

Young-Hyun Jin received the B.S. degree in mechanical engineering from the Korea Advanced Institute of Science and Technology (KAIST), Daejon, Korea, in 1998, and the M.S. degree in mechanical engineering from KAIST, Daejon, Korea, in 2000. He is currently pursuing the Ph.D. degree in KAIST. Since 2000, he has been working at the Digital Nanolocomotion Center as a Research Engineer. His research interests include optomechanical MEMS actuators and detectors for photon manipulation and biomedia processing.

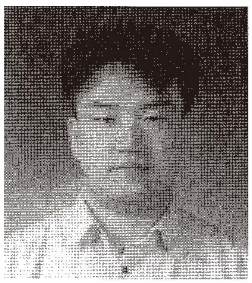

Moo-jin Choi received the B.S. degree from Busan National, Busan, Korea, in 1997 and the M.S. degree in mechanical engineering from the Korea Advanced Institute of Science and Technology (KAIST), Daejon, Korea, in 2000. He is currently working for the Korea Institute of Machinery and Materials as a researcher.

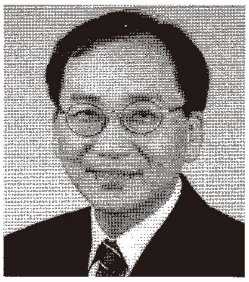

Young-Ho Cho received the B.S. degree *summa cum laude* from Yeungnam University, Daegu, Korea, in 1980; the M.S. degree from the Korea Advanced Institute of Science and Technology (KAIST), Seoul, Korea, in 1982; and the Ph.D. degree from the University of California at Berkeley for his electrostatic actuator and crab-leg microflexure research completed in December, 1990.
From 1982 to 1986 he was a Research Scientist of the CAD/CAM Research Laboratory, Korea Institute of Science and Technology (KIST), Seoul, Korea. From 1987 to 1991, he worked as a Post-Graduate Researcher (1987-1990) and a Post-Doctoral Research Associate (1991) of the Berkeley Sensor and Actuator Center (BSAC) at the University of California at Berkeley. In August 1991, Dr. Cho moved to KAIST, where he is currently an Associate Professor in the Departments of BioSystems & Mechanical Engineering as well as the Director of the Digital Nanolocomotion Center.
Dr. Cho's research interests are focused on the optomechanical and biofluidic MEMS with micro/nanoscaled actuators and detectors for photon manipulation and biomedia processing. In Korea, he has served as the Chair of the MEMS Division of the Korean Society of

Mechanical Engineers, the Chair of the Steering Committee of the Korea National MEMS Programs, the Chair of the Steering Committee of the Korean Next Generation Technology Development Program, the Leader of the Nanobio-Group in the National NanoForum and a member of the Committee of National Nanotechnology Planning Board. Dr. Cho has also served the international technical science community as the General Co-Chair of IEEE MEMS Conference 2003, a member of the Program Committee of IEEE Optical MEMS Conference, and the Chief Delegate of the Republic of Korea at the World Micromachine Summit. Dr. Cho is a member of IEEE and ASME.